NON-LINEAR PHASE RETRIEVAL COMBINED WITH ITERATIVE THRESHOLDING IN WAVELET COORDINATES

Valentina Davidoiu⋆, Bruno Sixou⋆, Max Langer⋆† and Françoise Peyrin⋆†

⋆ CREATIS, CNRS UMR5220 ; Inserm U630 ; INSA-Lyon ; Université Lyon 1; Université de Lyon, F-69621 Villeurbanne, France,
† European Synchrotron Radiation Facility, F-38043 Grenoble, France

ABSTRACT

With hard X-rays synchrotron beams, phase contrast can be obtained with the measurement of the Fresnel diffraction intensity patterns associated to a phase shift induced by the object. We have studied the resolution of this inverse problem with an iterative thresholding algorithm in wavelet coordinates combined with an iterative nonlinear method with a Tikhonov regularization. The phase retrieval algorithm was tested for a 3D Shepp-Logan phantom in the presence of noise. The results show that the combined approach outperforms the Mixed, the CTF and the nonlinear methods.

Index Terms— Inverse problems, Phase retrieval, X-ray imaging

1. INTRODUCTION

Phase sensitive imaging extends the possibilities of X-ray absorption imaging (μ-CT) [1] increasing the sensitivity, up to a factor 10^3 in the hard X-rays region. Coupled to tomography, it has found many applications in material science and biomedical imaging.

Several phase-sensitive imaging techniques have been developed [2, 3, 4]. In the propagation-based method, the detector is located behind the object, and several phase contrast images are recorded for different detector-sample distances [3]. The phase can be retrieved by methods based on the nonlinear relationship between the diffraction image and the phase map. Yet, this phase retrieval problem is ill-posed, so regularization approaches are required.

Several linear phase retrieval methods have already been proposed based on the Transport of Intensity Equation (TIE) [5], or the Contrast Transfer Function (CTF) [6]. The Mixed approach uses the two former methods [7]. These approaches rely on a linearized relation between the phase and the intensity. A new method based on a Tikhonov regularization and the Fréchet derivative of the intensity $I_D(\varphi)$ at different distances D was proposed recently [8].

Yet, these methods are rather sensitive to noise and the nonlinear approach fails to retrieve accurately the low frequencies of the phase map. It does not converge at all if the initialization point is too far from the solution. In this work, a novel approach is presented combining the former nonlinear iterative approach with a new low frequency regularized solution of the linear problem in wavelet coordinates.

This paper is organized as follows. In section 2, we summarize the image formation. In section 3 the resolution of the inverse problem in wavelet coordinates is detailed and the nonlinear approach with a Tikhonov regularization is also introduced. Experiments are performed to validate the proposed method in 4 and we conclude in section 5.

2. THE DIRECT PROBLEM OF IMAGE FORMATION

An object illuminated with partially coherent X-rays of wavelength λ can be described by the 3D complex refractive index distribution [9]:

$$n(x,y,z) = 1 - \delta_r(x,y,z) + i\beta(x,y,z) \tag{1}$$

where the imaginary part β describes the absorption index, while the real part δ_r is the refractive index decrement for the spatial coordinate (x,y,z). The propagation path of the X-ray in a thin object can be presumed straight, so the interaction of X-rays with matter can be described by a transmittance function T of the coordinates $\mathbf{x} = (x,y)$ in a plane perpendicular to the propagation direction z [9]:

$$T(\mathbf{x}) = \exp[-B(\mathbf{x}) + i\varphi(\mathbf{x})] = a(\mathbf{x})\exp[i\varphi(\mathbf{x})] \tag{2}$$

where $a(\mathbf{x})$ is the amplitude modulation and $\varphi(\mathbf{x})$ is the phase shift induced by the object. B and φ are related to the real and imaginary part of the index by:

$$B(\mathbf{x}) = \frac{2\pi}{\lambda}\int \beta(x,y,z)dz \tag{3}$$

and

$$\varphi(\mathbf{x}) = -\frac{2\pi}{\lambda}\int \delta_r(x,y,z)dz. \tag{4}$$

The recorded intensity at distance D is given by the squared modulus of the Fresnel transform of the transmittance:

$$I_D(\mathbf{x}) = |\mathcal{F}r_D\left[T(\mathbf{x})\right]|^2 = |T(\mathbf{x}) * P_D(\mathbf{x})|^2 \tag{5}$$

where $*$ denotes the 2D convolution of the transmittance with the Fresnel propagator at distance D,

$$P_D(\mathbf{x}) = \frac{1}{i\lambda D} \exp\left(i\frac{\pi}{\lambda D}|\mathbf{x}|^2\right). \quad (6)$$

3. THE PHASE RETRIEVAL INVERSE PROBLEM

The image formation is a highly nonlinear process. Assuming that the absorption is slowly varying, several phase retrieval approaches have linearized the Eq. 5 under some rather restrictive assumptions. The Fourier transforms of the intensity can be written [7]:

$$\mathcal{F}\{I_D\}(\mathbf{f}) = \tilde{I}_D^{\varphi=0}(\mathbf{f}) + 2\sin(\pi\lambda D|\mathbf{f}|^2)\mathcal{F}\{I_0\varphi\}(\mathbf{f}) + \frac{\lambda D}{2\pi}\cos(\pi\lambda D|\mathbf{f}|^2)\mathcal{F}\{\nabla\cdot(\varphi\nabla I_0)\}(\mathbf{f}) \quad (7)$$

where $I_D^{\varphi=0}(\mathbf{f})$ is the intensity at distance D if the phase was zero. The absorption $a(\mathbf{x})$ is obtained experimentally if the detector is placed at distance $D = 0$ m from the sample. Based on the former equation, the phase retrieval problem can be express as an inverse linear problem:

$$\mathcal{I} = \mathcal{B}\varphi + \varepsilon, \quad (8)$$

where $\mathcal{I} = I_D - I_D^{\varphi=0}$ is the noisy data, ε additive Gaussian noise, φ the phase to be retrieved and $\mathcal{B}$ is a linear operator. This solution is not optimal and gives not good reconstructions for noisy data and low frequencies.

In this work, in order to improve the phase retrieval, we have combined two approaches: a resolution of the linear problem in wavelet coordinates with an iterative thresholded Landweber type algorithm [10, 11, 12] and a nonlinear approach based on the Fréchet derivative of the intensity. The phase maps where the Mixed approach or the CTF method stagnate will be used as an initialization in our method. The linear methods provide in very few iterations an approximate solution but improved performance requires to take into account the non linearities and a low frequency wavelet denoising, with a slower convergence rate.

3.1. Resolution of the linear inverse problem in wavelet coordinates

In this section, we consider a resolution approach for the inverse problem based on the orthogonal wavelet representation and a classical thresholded Landweber algorithm. We suppose that the phase φ admits a sparse representation in a orthogonal wavelet base $\Psi = \{\psi_\lambda, \lambda \in \mathcal{I}\}$, which is written:

$$\varphi = \mathcal{W}^*\mathbf{v}, \quad (9)$$

where $\mathbf{v} \in l_2$ is a wavelet coefficients vector, and $\mathcal{W}^*$ is the synthesis operator. The corresponding family is indexed by the elements λ of an infinite set $\mathcal{I}$, which includes the level of the resolution, the position and the type of wavelet.

The phase retrieval problem can be formulated as an unconstrained optimization problem with an l_1 regularization term for the wavelet coefficients and with a regularization parameter κ. The wavelet coefficients are optimized as follows:

$$\min\left\{\frac{\|\mathcal{I} - \mathcal{B}\mathcal{W}^*\mathbf{v}\|_2^2}{2} + \kappa\|\mathbf{v}\|_1, \mathbf{v} \in l_2\right\} \quad (10)$$

where l_p is the norm of the vector $\mathbf{v}$ defined as: $\|\mathbf{v}\|_p = (\sum_i v_i^p)^{1/p}$.

In terms of convex analysis, the first term is convex, semi-continuous and differentiable with β-Lipschitz continuous gradient for a coefficient $\beta > 0$. The regularizing term is semi-continuous and not differentiable. This optimization problem has been studied and efficient algorithms have been proposed [12].

We selected the following iterative method: $\mathbf{v}_0 \in l_2$, and $0 < \tau < 2/\beta$ and for each $n \in N$, we construct the following sequence:

$$\mathbf{v}_{n+1} = \mathcal{S}_{\alpha\tau}\{\mathbf{v}_n - \tau\mathcal{W}\mathcal{B}^*[\mathcal{B}\mathcal{W}^*(\mathbf{v}_n)] - \mathcal{I}\} \quad (11)$$

where $\mathcal{S}_a(u) = \mathtt{sign}(u)\max(|u| - a, 0)$ is the soft thresholding operator. The solution is obtained from the final iterate $\mathbf{v}_\infty$ with $\varphi_\infty = \mathcal{W}^*\mathbf{v}_\infty$. Since we intend to use the wavelets to improve the low frequency phase retrieval, the iterations described by Eq. 11 are implemented only at the lowest level of resolution and the operator $\mathcal{W}\mathcal{B}\mathcal{W}^*$ is approximated with the lowest level of resolution of the wavelet basis.

The solution obtained when the error stagnates is used as initialization for the nonlinear approach based on the Fréchet derivative of the intensity with Tikhonov regularization described in the next section. When the nonlinear solution stagnates, the linear wavelet algorithm is used again. By alternating the two phase retrieval approaches, we obtain a progressive refinement of the solution.

3.2. Nonlinear phase retrieval with Tikhonov regularization

This regularization methodology is more general that the one investigated in [8] and it gives goods results for noisy and non smooth phase maps. The intensity I_D can be considered as a continuous and a nonlinear function of the phase φ. We have assumed that the domain $\mathcal{D}[I_D(\varphi)]$ where the operator $I_D(\varphi)$ is defined belongs to the functional Sobolev space $H_\diamond^{2,2}(\Omega) = \{\varphi \in H^{2,2}(\Omega),\ \frac{\partial\varphi}{\partial\vec{n}} = 0\}$, where $\frac{\partial\varphi}{\partial\vec{n}}$ is the normal derivative of the phase [8]. The aim of the nonlinear Tikhonov regularization is to minimize the functional:

$$J_\alpha(\varphi) = \frac{1}{2}\|I_D(\varphi) - I_\delta\|_{L_2(\Omega)}^2 + \frac{\alpha}{2}\|\varphi\|_{L_2(\Omega)}^2 \quad (12)$$

where α is a regularization parameter, and where $\|.\|_{L_2(\Omega)}$ denotes the $L_2(\Omega)$ norm. The nonlinear Tikhonov regularization has been extensively studied. The optimality condition

can be written with the adjoint $I_D^{'}(\varphi)^*$ of the Fréchet derivative of the intensity $I_D^{'}(\varphi)$:

$$\left\langle I_D^{'}(\varphi)^*[I_D(\varphi) - I_\delta], h \right\rangle_{L_2(\Omega)} + \alpha\langle\varphi, h\rangle_{L_2(\Omega)} = 0 \quad (13)$$

where $\langle , \rangle$ denotes the scalar product. Let φ_k be the phase at the iteration k. The phase estimate φ_{k+1} at the iteration $k+1$ is obtained from the phase φ_k at the previous iteration k with:

$$\varphi_{k+1} = \varphi_k - \tau_k\{I_D^{'}(\varphi_k)^*[I_D(\varphi_k) - I_\delta] + \alpha\varphi_k\} \quad (14)$$

To minimize the nonlinear Tikhonov's functional, along the descent direction:

$$\delta_k = I_D^{'}(\varphi_k)^*[I_D(\varphi_k) - I_\delta] + \alpha\varphi_k, \quad (15)$$

a step length parameter τ_k is chosen. The standard Landweber method is thus modified by introducing a linear search procedure with a variable step τ_k, obtained with a dichotomy strategy. The regularizing parameter α is chosen by trial-and-error in order to obtain the best decrease of the regularization functional.

The computation of the iterates is based on the calculation of the adjoint of the Fréchet derivative of the intensity. The Fréchet derivative of the operator $I_D(\varphi_k)$ at the point φ_k is the linear operator G_k defined as [8]:

$$I_D(\varphi_k + \varepsilon) = I_D(\varphi_k) + G_k(\varepsilon) + O(\varepsilon^2). \quad (16)$$

$I'_D(\varphi_k)(\varepsilon) = G_k(\varepsilon)$ is a linear operator and it is computed explicitly together with the adjoint operator G_k^* in [8].

4. SIMULATIONS DETAILS

4.1. Simulation of the image formation

The imaging system was simulated in a deterministic fashion [13]. Two phantoms were defined, one for the absorption coefficient and one for the refractive index decrement. Fig. 1(a) displays the 3D Shepp-Logan, consisting of a series of ellipsoids on which the projections are based. In order to perform realistic simulations, the values of the absorption coefficient δ and of the refractive index β for different materials were used in different regions [13].

The intensity images are obtained as the squared modulus of the convolution product calculated by Fourier transforms, using Eq. 5. The intensity images were calculated for the three propagation distances D=[0.035, 0.072, 0.222]m. Fig. 1(b) displays the intensity image obtained at the first distance with 24dB. These propagation distances are taken into account randomly during the phase retrieval algorithm. The X-ray energy was 24 keV ($\lambda = 0.5166\mathring{A}$) and the corresponding pixel size was 1μm. The images were down-sampled to 512×512 pixels.

The simulations in this work were performed for additive uniformly distributed white noise with zero mean and with a peak-to-peak signal to noise ratios (PPSNR) of 24dB. The peak-to-peak signal to noise ratio is defined by: $PPSNR = 20\log(\frac{f_{max}}{n_{max}})$, where f_{max} is the maximum signal amplitude and n_{max} is the maximum noise amplitude. Similar results were obtained for PPSNR below 12dB.

4.2. Initialization, stopping rules and wavelet implementation

In our simulations, the Mixed and the CTF methods were used because they provide in very few iterations approximate initialization solutions. These phase maps are stagnation points where the novel approach is necessary. An important role in the algorithms is played by the regularization parameters. In order to avoid obtaining solutions diverging far away from the real solution, these parameters are chosen by trial-and-error. The parameter in the Mixed approach may be set at a very small value (i.e 10^{-100}), and in the proposed algorithm α and κ are set to the same value 10^{-3}. The iterations are terminated when the following conditions are fulfilled:

$$\|I_D(\varphi_{k+1}) - I_D(\varphi_k)\|_{L_2(\Omega)} \leq \omega\|I_D(\varphi_k)\|_{L_2(\Omega)} \quad (17)$$

$$\|I_\delta - I_D\|_{L_2(\Omega)} \geq \delta \quad (18)$$

where ω is a parameter that was set at 0.01 by trial-and-error.

For the wavelet representation, the orthonormal wavelet $DB1$ Dauchechies implemented in Matlab was used with only 64 low resolution coefficients. Similar results were obtained with other wavelet basis. The convex part of the functional to be minimized is differentiable with Lipschitz gradient with $\beta = \|\mathcal{W}\mathcal{B}\mathcal{W}^*\|^2$. Following the approach

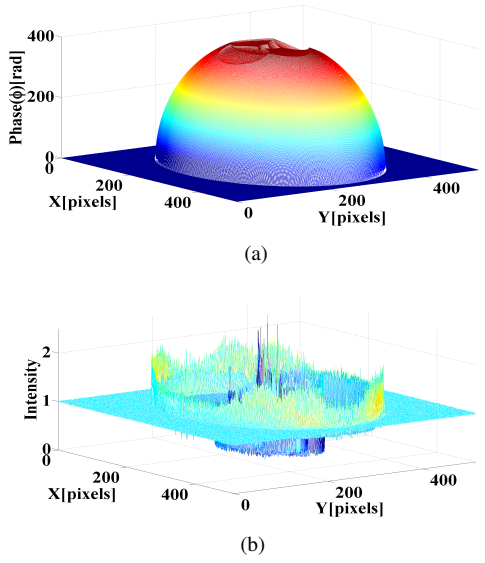

Fig. 1. (a) Original phase map to be retrieved, (b) Fresnel diffraction pattern at propagation distance $D = 0.035$ m with PPSNR=24dB.

proposed in [14], given $\mathbf{x}_0$ et $\mathcal{C} = \mathcal{W}\mathcal{B}\mathcal{W}^*$, we construct a sequence $(\mathbf{x}_n)$ such that $\mathbf{x}_n = \mathcal{C}^*\mathcal{C}\mathbf{x}_{n-1}$, and at each iteration $\rho_n = \frac{\|\mathbf{x}_n\|}{\|\mathbf{x}_{n-1}\|}$ is calculated. After convergence, $\lim_{n\to\infty} \rho_n = \rho_\infty = \|\mathcal{W}\mathcal{B}\mathcal{W}^*\|^2$.

Since ideal reconstruction is available, direct comparisons can be made. The method will be quantitatively evaluated by measuring the normalized mean square error (NMSE) using the $L_2(\Omega)$ norm. It is defined by: $NMSE = 100 \times \frac{\|\varphi-\varphi_k\|_{L_2(\Omega)}}{\|\varphi\|_{L_2(\Omega)}}$, where φ_k is the phase recovered at iteration k and φ the ideal phase to be recovered.

5. DISCUSSION AND CONCLUSION

The performance of the proposed method was analyzed by comparison with the solutions obtained for noisy data with the CTF [6] and the Mixed approach [13].

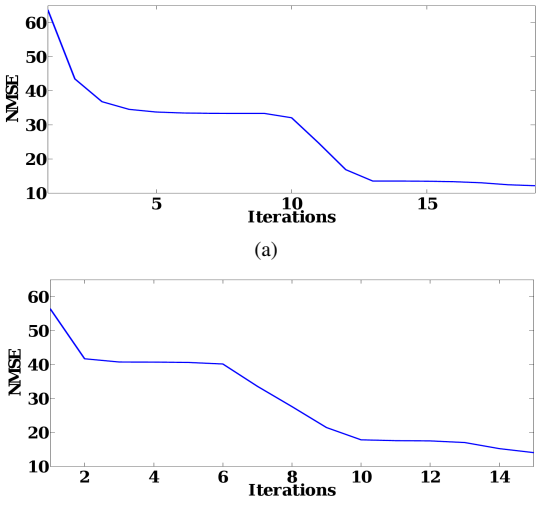

Fig. 2. Normalized mean square error for the phase versus iteration number with the proposed algorithm initialized with (a) the Mixed solution and (b) with the CTF solution.

The evolution of the NMSE as a function of the iteration number is displayed in Fig. 2 for the two starting points. In these plots, one iteration corresponds to a random cycle through the intensity images obtained for the three distances. These curves show the refinement of the solution obtained with the combined WNL approach. The wavelet denoising scheme makes possible the escape from the local minima obtained with the nonlinear method alone [8]. The error maps for noisy data are displayed in Fig. 3.

A comparison between the true solution for the Shepp Logan phantom and the solutions obtained with the three approaches, CTF, Mixed and Wavelet-Nonlinear (WNL), is showed in Fig. 4. The errors on the phase map have been significantly reduced by our new method. According to the results presented in Table 1, an error decrease of a 80.95% and 75.15% was obtained for the Mixed and the CTF solutions respectively. The phases used as starting points for our reconstruction are displayed in Fig. 5(a), 5(b), together with the corresponding phases retrieved with the proposed algorithm Fig. 5(c), 5(d).

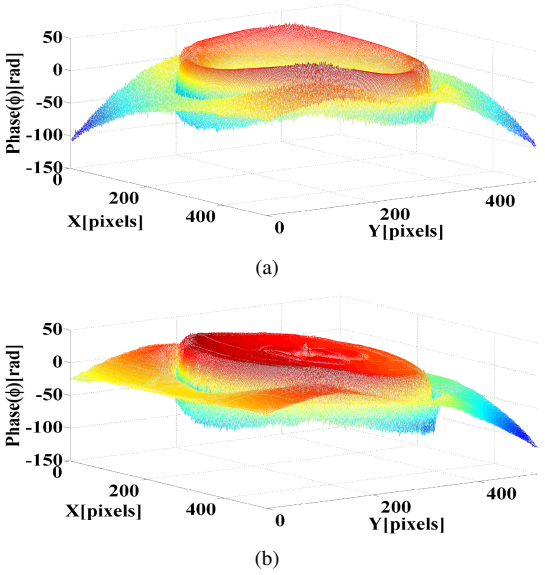

Fig. 3. Error map for the phase retrieved with the proposed algorithm initialized with (a) the Mixed solution and (b) with the CTF solution.

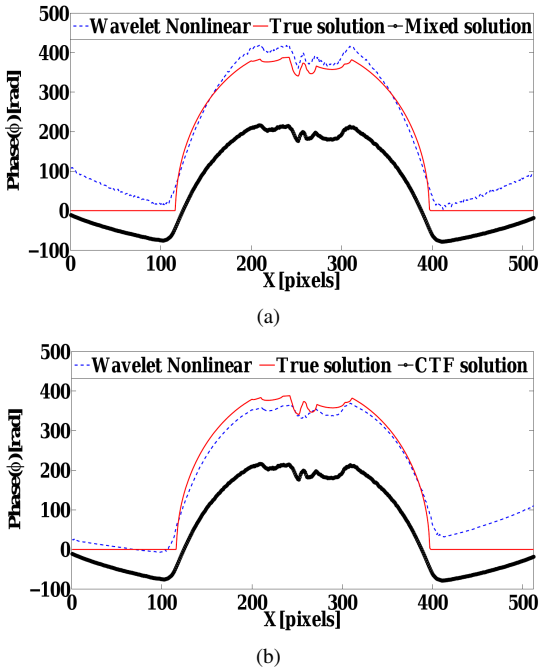

Fig. 4. Diagonal profiles obtained for the true, the Mixed, the CTF solutions and the solution obtained with the combined nonlinear and wavelet approach.

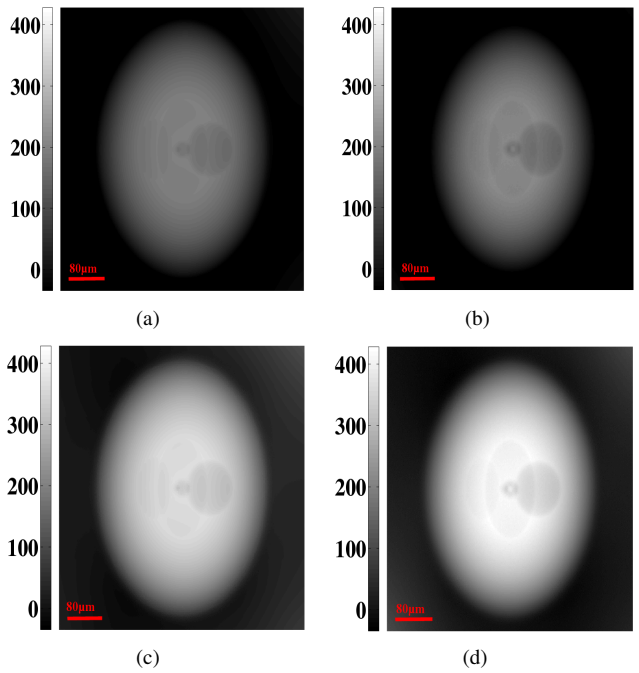

Fig. 5. Phase solutions obtained with the (a) Mixed and (b) CTF algorithms and reconstructed phase with the proposed algorithm for the starting point given by (c) Mixed and (d) CTF algorithms.

Table 1. Initial NMSE(%) and values at convergence for Wavelet-Nonlinear method (WNL) for the two initializations.

CTF	WNL	Mixed	WNL
56.54	14.05	63.84	12.16

In this work, we have presented a new phase retrieval approach based on a combination of a nonlinear phase retrieval method with the Fréchet derivative of the intensity and a thresholded Landweber algorithm in wavelet coordinates. Both the high and low frequency ranges of the phase retrieved are improved. Three propagation distances are used in a random way to achieve a good reconstruction. The reconstruction quality for a projection of a 3D Shepp-Logan phantom has been quantitatively evaluated with noise. The combined method outperforms the linear methods. In future work, the method will be tested on experimental data to test its robustness to noises and artifacts. The method is expected to open new perspectives for the study of biological samples.

6. REFERENCES

[1] A. Momose, T. Takeda, Y. Itai and K. Hirano,"Phase-contrast X-ray computed tomography for observing biological tissues," Nat. Med., **2,** 473–475 (1996).

[2] U. Bonse and M. Hart,"An X-ray interferometer," Appl. Phys. Lett., **6,** 155-156 (1965).

[3] S.W. Wilkins, T.E. Gureyev, D. Gao, A. Pogany and A.W. Stevenson, "Quantitative phase imaging using X-rays,"Phys.Rev.Lett., **77**, 2961–2964, (1996).

[4] T. Weitkamp, A. Diaz, C. David, F. Pfeiffer, M. Stampanoni, P. Cloetens and E. Ziegler,"X-ray phase imaging with a grating interferometer," Opt. Express, **13,** 6296–6304 (2005).

[5] D. M. Paganin,"Coherent X-ray Optics," Oxford University Press, New York (2006).

[6] P. Cloetens, R. Barrett, J. Baruchel, J. P. Guigay and M. Schlenker,"Phase objects in synchrotron radiation hard X-ray imaging," J. Phys. D.:Appl. Phys. **29,** 133–146 (1996).

[7] J. P. Guigay, M. Langer, R. Boistel, and P. Cloetens,"A mixed contrast transfer and transport of intensity approach for phase retrieval in the Fresnel region," Opt. Lett. **32,** 1617-1619 (2007).

[8] V. Davidoiu, B. Sixou, M. Langer and F. Peyrin, "Non-linear phase retrieval based on Fréchet derivative," Opt.Express **19,** 22809–22819 (2011).

[9] M. Born and E. Wolf,"Principles of Optics," Cambridge University Press (1997).

[10] E. J. Candes, J. Romberg and T. Tao," Robust uncertainty principles: exact signal reconstruction from highly incomplete frequency information,"IEEE Trans. Inf. Theory, **52**, 489–509, (2006).

[11] I. Daubechies, M. Fornasier, and I. Loris,"Accelerated projected gradient method for linear inverse problems with sparsity constraints," JFAA, **14,** 764-792 (2008).

[12] F. Dupe, J.M. Fadili and J.L. Starck,"A proximal iteration for deconvolving poisson noisy images using sparse representations,"IEEE Trans. Image Process., **18,** 310–321 (2009).

[13] M. Langer, M. Cloetens, J.P. Guigay and F. Peyrin,"Quantitative comparison of direct phase retrieval algorithms in in-line phase tomography,"Med.Phys., **35,** 4556–4565, (2008).

[14] L. Chaari, N. Pustelnik, C. Chaux and J.C. Pesquet,"Solving inverse problems with overcomplete transforms and convex optimization techniques," SPIE San Diego, Californie, USA (2009).